DEFENSE TECHNICAL INFORMATION CENTER

Information for the Defense Community

DTIC® has determined on 07/16/2010 that this Technical Document has the Distribution Statement checked below. The current distribution for this document can be found in the DTIC® Technical Report Database.

☒ **DISTRIBUTION STATEMENT A.** Approved for public release; distribution is unlimited.

☐ **© COPYRIGHTED**; U.S. Government or Federal Rights License. All other rights and uses except those permitted by copyright law are reserved by the copyright owner.

☐ **DISTRIBUTION STATEMENT B.** Distribution authorized to U.S. Government agencies only (fill in reason) (date of determination). Other requests for this document shall be referred to (insert controlling DoD office)

☐ **DISTRIBUTION STATEMENT C.** Distribution authorized to U.S. Government Agencies and their contractors (fill in reason) (date of determination). Other requests for this document shall be referred to (insert controlling DoD office)

☐ **DISTRIBUTION STATEMENT D.** Distribution authorized to the Department of Defense and U.S. DoD contractors only (fill in reason) (date of determination). Other requests shall be referred to (insert controlling DoD office).

☐ **DISTRIBUTION STATEMENT E.** Distribution authorized to DoD Components only (fill in reason) (date of determination). Other requests shall be referred to (insert controlling DoD office).

☐ **DISTRIBUTION STATEMENT F.** Further dissemination only as directed by (inserting controlling DoD office) (date of determination) or higher DoD authority.

Distribution Statement F is also used when a document does not contain a distribution statement and no distribution statement can be determined.

☐ **DISTRIBUTION STATEMENT X.** Distribution authorized to U.S. Government Agencies and private individuals or enterprises eligible to obtain export-controlled technical data in accordance with DoDD 5230.25; (date of determination). DoD Controlling Office is (insert controlling DoD office).

Threshold Damage of *In Vivo* Porcine Skin at 2000 nm Laser Irradiation

Bo Chen, MS,[1] Daniel C. O'Dell, BS,[1] Sharon L. Thomsen, MD,[1] Benjamin A. Rockwell, PhD,[2] Ashley J. Welch, PhD[1]

[1] Biomedical Engineering Laser Laboratory, University of Texas at Austin, Austin, Texas 78712
[2] Air Force AFRL/HEDO, Brooks City-Base, Texas 78235

A series of experiments were conducted *in vivo* on female Yucatan mini-pigs to determine the ED_{50} damage thresholds for 2000 nm continuous wave laser irradiation. These results provide new information for refinement of Maximum Permissible Exposure (MPE). The study employed Gaussian laser beam exposures with spot diameters ($1/e^2$) of 4.83 mm, 9.65 mm and 14.65 mm and exposure durations of 0.25 s, 0.5 s, 1.0 s and 2.5 seconds as a function of laser power. The effect of each irradiation was evaluated within one minute after irradiation and the final determination was made at 48 hours post exposure. Probit analysis was conducted to estimate the dose for 50% probability of laser-induced damage (ED_{50}) defined as persistent redness at the site of irradiation for the mini-pig skin after 48 hours. Histopathologic procedures were used to determine the mechanisms of the laser effects in the skin and map the extent and severity of the lesions. The thresholds study shows that consideration for lowering the current Maximum Permissible Exposure (MPE) limits should be explored as the laser beam diameter becomes larger than 3.5 mm. Based on the limited experimental data, the duration and size dependences of the ED_{50} damage thresholds could be described by an empirical equation: $Irradiance\ at\ the\ threshold[J/cm^2] = (5.669 - 1.81 \times spot\ diameter[cm]) \times exposure\ duration[s]^{-0.794}$.

Key words: Gaussian laser irradiation; laser injury; laser safety; Maximum Permissible Exposure (MPE); skin damage; visible lesion; Yucatan mini-pig

1 INTRODUCTION

Laser systems operating in the wavelength around 2000 nm are in widespread use in military, medical, and industrial applications. Being relatively new to the medical fields, the Q switch and long pulse Ho:YAG lasers (λ=2.1 μm) are principally used to precisely ablate bone and cartilage, with many applications in orthopedics for arthroscopy [1-3], urology for lithotripsy (removal of kidney stones) [4-6], otolaryngology for endoscopic sinus surgery [7-9], and spine surgery for endoscopic disc removal [10]. With the recent development of continuous-wave systems at 2000 nm, it may be necessary to evaluate the need to refine the existing laser safety limiting exposure limits for these systems.

Maximum Permissible Exposure (MPE) is the level of radiation to which a person may be exposed without hazardous effect or adverse biological changes in the eyes and skin [11]. The MPEs for various wavelengths and pulse widths are defined by the American National Standards Institute (ANSI). This determination is done by the experts on the bioeffects subcommittee upon evaluation of minimum visible lesion threshold data, modeling and understanding of the mechanisms for damage. The ANSI Z136.1-2000, American National Standard for Safe Use of Lasers [11] for skin at wavelengths between 1.8 μm and 2.6 μm and laser exposures from 1.0 ms to 10.0 s (see Table 1) is based on very little experimental data [12,13]. In this wavelength regime, the limited experiments have investigated cornea epithelial damage thresholds for exposure duration less than 0.25 s and laser spot size smaller than 1.8 mm.

TABLE 1. Maximum Permissible Exposure (MPE) for Skin Exposure to a Laser Beam (From ANSI Z136.1-2000)[11]

Wavelength(μm)	Exposure Duration, t (s)	MPE (J cm^{-2})	Limit Aperture Diameter (mm)
1.800 to 2.600	10^{-3} to 10	$0.56\ t^{0.25}$	3.5

t is the laser exposure duration.

Studies on laser safety evaluate the MPE of the eye and the skin to laser irradiations. It is typically a factor of ten below the ED_{50} damage threshold [14]. Exposure to levels at the published MPE values for the eye and skin may be "uncomfortable" [11]. Thus, it is good practice to maintain exposure levels sufficiently below the MPE to avoid discomfort [11]. In an effort to provide additional data for 2000 nm laser safety standards, a series of experiments and tests were conducted on Yucatan mini-pigs to determine various parameters that inflict threshold damage on skin at

Optical Interactions with Tissue and Cells XVII, edited by Steven L. Jacques, William P. Roach,
Proc. of SPIE Vol. 6084, 60840C, (2006) · 1605-7422/06/$15 · doi: 10.1117/12.639069

2000 nm for large spot sizes (5 mm ~ 15 mm). Thresholds were determined in terms of the minimum visible lesion for exposure durations from 0.25 second to 2.5 seconds.

The formation of thermally induced lesions in skin is a temperature-time rate process that is associated with the thermal denaturation of proteins [15]. The process begins with the local absorption of laser light in skin that is converted to heat. The localized heat source S [W/cm^3] at position r(x,y,z) and time t is a function of the local wavelength dependent absorption coefficient μ_a[1/cm] of the laser light

$$S(r,t) = \mu_a(r)\phi(r,t), \tag{1}$$

where $\phi(r,t)$ [W/cm^2] is the fluence rate at position r(x,y,z) and time t. The primary absorbers, chromophores, for visible light and near IR radiation in skin are blood and melanin in the pigment epithelium. At 2000 nm, water becomes the primary chromophore. Temperature $T(r,t)$ resulting from the absorbed laser light is governed by heat generation, storage, diffusion and perhaps blood perfusion for long laser exposures. The actual pattern of light absorption is governed by light scattering at visible and near IR wavelengths; However at wavelength above 1.4 μm where scattering is insignificant, light propagation can be described by Beer's law. When $\mu_a(r) = \mu_a$:

$$S(r,t) = \mu_a(1-r_s)E(x,y,t)e^{-\mu_a z}, \tag{2}$$

where $E(x,y,t)$ [W/cm^2] is the irradiance and r_s is the specular reflectance from the skin surface[16].

The animal model that best represents black human skin is the Yucatan mini-pig. It is anatomically similar to all human skin than the commonly used Yorkshire model [17]. The skin of the Yucatan mini-pig has less hair and increased density of melanin granules relative to the Yorkshire pig. The Yucatan mini-pig has dark skin color and statistically, the flank skin thickness is approximately close to that of human face, arm, and neck skin, which have high probability of accidental exposure. By using this model, the properties of the human skin can be more closely approximated to gain a better understanding of human laser-tissue interaction for the wavelength of interest.

2 MATERIAL AND METHODS

Animal Preparation

The animal use protocol was approved by the Institutional Animal Care and Use Committee at the University of Texas at Austin. Six female Yucatan mini-pigs, weighing between 24.3 to 34.8 kg, were used in this study. Before beginning each of the experiments, the mini-pig was anesthetized initially with IM Telazol-Ketamine-Xylazine(TKX) and intubated. Isoflurane (1~3%) was administered for anesthesia maintenance throughout the procedure by a certified registered laboratory animal technologist. Heart rate, SpO_2 and respiration were monitored throughout the experiment. In addition, Rimadyl (Carprofen) was given at the end of procedure to alleviate possible post surgical pain. After the mini-pig was anesthetized, its hair was removed using Nair® depilatory. Nair® was removed five minutes after application and the mini-pig skin was bathed with Betadine and then water. The mini-pig was marked with a metallic-silver permanent marker to make grids for identification and location of the numerous irradiation sites. The dimensions of the grids depended upon the laser spot size.

Experimental Setup

A rack mountable fiber optic CW laser (IPG Photonics Corporation) with a maximum 20 W output at a wavelength 2000 nm was used to create an array of irradiations. The output power was adjusted by changing the current on the front panel display. A power meter EPM2000 (Molectron Detector Inc., Portland, OR) with air-cooled power meter probes PM30 or PM150 (Molectron Detector Inc., Portland, OR) was used to measure the output power corresponding to each current setting. Telescopes were employed to generate a collimated laser beam with desired spot diameters. A pulse generator (DG535, Stanford Research Systems) was used to trigger laser output and control the exposure durations. The pulse generator also triggered a function generator (HP 33120A, Hewlett-Packard Company), which controlled the imaging rate of an IR array detector thermal camera (Phoenix^{TM} DAS camera system, Indigo, CA). The IR camera began capturing infrared images 0.1 second before the laser irradiation on the mini-pig skin, and

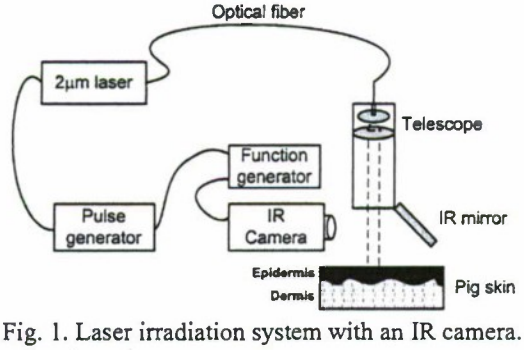

Fig. 1. Laser irradiation system with an IR camera.

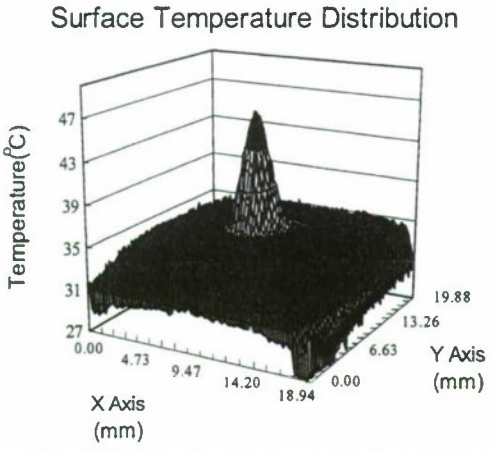

Fig. 2 Skin surface temperature distribution after 30 ms laser irradiation.

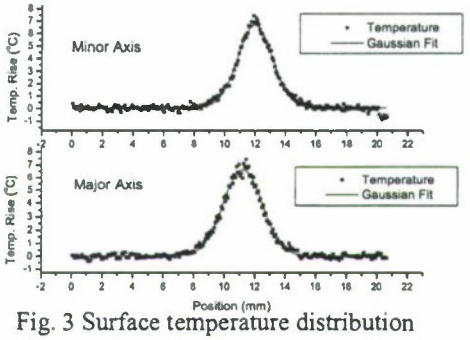

Fig. 3 Surface temperature distribution along major and minor axes after 30 ms laser irradiation.

continued recording for 4 ~ 9 seconds after the laser was turned off. The IR camera imaging rate was set at 100 frames per second. The measurement system was arranged as depicted in Figure 1. Temperature calibration for the IR camera was done by using a blackbody heat source after laser irradiations on pig skin. The telescope and IR mirror were both mounted on the IR camera to ensure all burn sites were located at a fixed distance from the laser for the same spot size.

Three different laser spot sizes were produced by various telescopes. The laser beam profiles were measured using the knife-edge method [18] before conducting the mini-pig experiment, and were confirmed by spatial IR imaging on skin for a 30 ms laser irradiation. The light 1/e penetration depth of skin at 2000 nm was approximately 200 μm and the associated characteristic thermal diffusion time for a large spot diameter was about 300 ms. Compared to the characteristic diffusion time of skin, heat conduction within the 30 ms pulse duration was quite small and insignificant. The temperature rise was directly proportional to the irradiance [W/cm^2] for the case of no heat transfer during the laser pulse. Therefore, the measured surface temperature distribution (Fig. 2) obtained from a thermal camera represented the spatial intensity profile of the nominally Gaussian shape laser beam with 1/e^2 diameters of about 5 mm. The spatial profile was elliptic rather than circular, deviating in radius by about 10% along the major and minor axes. The radial profiles along the two axes of the elliptic laser beam (see Fig.3) were essentially Gaussian in shape with 1/e^2 diameter 5.10 mm and 4.66 mm. The arithmetic average of the two radii was 4.88 mm which was very close to the knife-edge measurement value 4.83 mm. The spatial profiles of two larger laser beam sizes created with various telescopes were measured by using spatial IR imaging as well as knife-edge method. The diameters values of 9.65 mm and 14.65 mm measured by knife-edge method were close to measurement values 10.08 mm and 13.84 mm derived from IR imaging respectively deviating by about 5%. The differences of these two methods were due to the elliptic rather than circular spatial profile assumed by the knife-edge measurement and by slight curvature of the mini-pig skin surface.

Experimental Procedures

Radiant exposures were made at specified exposure durations of 0.25 sec, 0.5 sec, 1 sec, and 2.5 seconds for spot diameters of 4.83 mm, 9.65 mm, and 14.65 mm. The number of irradiations for each of the 12 spot size-exposure conditions was 19 ~ 37 with an average of 27 per condition. The variation in laser power provided sufficient data points for probit analysis of damage/no damage response as a function of power. Forty-eight hours after laser irradiation, the size and type of lesions were observed and photographed by a digital camera (C-3040, Olympus Optical Co., Ltd., Japan) in order to find the ED_{50} damage threshold for the spot size-exposure conditions.

Tissue Specimens Preparation

Forty-eight hours after irradiation, mini-pigs were euthanized. Tissue specimens of each lesion were taken and fixed in 10% neutral buffered formalin, embedded with paraffin, sectioned and stained with hematoxylin and eosin (H&E). Serial consecutive sections were cut through the sample blocks to locate the center of the thermal lesion at the microscopic level and determine the maximum diameter of the lesion in skin.

3 RESULTS

ED_{50} Damage Threshold Determination

To determine different degrees of damage and to choose a reliable and reproducible threshold of minimal visual laser-induced damage, a pilot study was conducted on a Yucatan mini-pig to generate damages from no visible lesion to tissue ablation and charring. Based on the 48-hours post exposure reading, we defined the threshold thermal damage as grossly apparent persistent redness of the skin at the irradiation site at 48 hours. This kind of lesion was characterized as second-degree burn. Lesions around persistent redness threshold initially appeared as red, flat spots on the skin at the site of irradiation. Most of the lesions appeared instantly within 1 min of the onset of laser irradiation on the skin. At some specific power level near the estimated persistent redness threshold, redness developed on the skin several minutes after the laser irradiation took place and persisted in the 48-hours post reading. Moreover, several instant red spots recorded immediately after irradiations were not observed at the 48-hours post reading.

More severe damage included epidermal roughening, blistering and whitening coagulation of the underlying dermis. Based on visible skin damage/no damage (i.e. persistent redness), probit analysis was used to determine the ED_{50} damage threshold. Probit analysis [19, 20] provided a statistically-estimated dose for 50% probability of minimal visual laser-induced damage (ED_{50}) for the mini-pig skin. Data points (damage/no damage for each condition) were entered into the probit statistical analysis package (Lund, B., Probit Fit Dose-Response Data Analysis Program, Version 1.02, U.S. Army Medical Research and Material Command, Hazards Research Branch) and the ED_{50} was calculated along with fiducial limits at the 95% confidence level.

In order to truly evaluate laser damage thresholds, average irradiance [W/cm^2] or radiant exposure [J/cm^2] reported in this paper was calculated as the applied laser power or energy divided by the $1/e^2$ spot area rather than 1/e spot area which is used in the laser safety classification. In fact, the peak irradiance or radiant exposure for our near Gaussian profile was twice the average value. Peak values were not reported.

Probit analyses [19,20] were conducted to estimate ED_{50} thresholds according to two different end points of thermal lesions, 1) instant redness observed on skin within 1 min after laser irradiation and 2) persistent redness at the site 48 hrs after irradiation.

The laser power for ED_{50} thresholds at 1 min and 48-hours post exposure readings are compared in Table 2. Standard deviation (σ) was derived from the probit fit curve by the definition:

$$\sigma = (ED_{84} - ED_{16})/2, \quad (3)$$

where ED_{84} represented the dose for 84% probability of laser-induced damage, and similarly for ED_{16}. At some irradiation conditions, direct estimations were made without using probit analysis, because the data was quite consistent and there was insufficient scatter for the probit program. In other words, there was consistently damage or no damage above or below a specific exposure level (P_{da} and P_{no} respectively). In these limited cases, the ED_{50} value was estimated as the middle point between the lowest value consistent damage (P_{da}) and largest value of no damage (P_{no}). The standard deviation of ED_{50} value was equal to 32% of the border width (P_{da}- P_{no}).

Even though the Yucatan mini-pig skin best represents human skin, the dark pigmentation of the skin hindered the visual determination of threshold damage, and therefore could have contributed to inflation in the ED_{50} value due to observational threshold differences. Other experimental uncertainties are mainly from the power measurements. The air-cooled power meter probes PM30 and PM150 have 3% uncertainties, and the power meter EPM2000 has 1% read-out error. However, these instrumental errors are relatively small to the uncertainty from visual damage determination.

TABLE 2. The ED_{50} Power and Standard Deviation at Damage Thresholds Defined as Instant Redness within One Minute or Persistent Redness after 48 hours.

Diameter (mm) / Duration(s)	4.83		9.65		14.65	
	Instant (W) *	Persistent (W) **	Instant (W)	Persistent (W)	Instant (W)	Persistent (W)
0.25	2.12 ± 0.92	$2.62 \pm 0.28^{\#}$	7.73 ± 0.62	8.46 ± 1.04	11.79 ± 1.55	16.09 ± 0.43
0.5	1.72 ± 0.38	1.49 ± 0.48	2.93 ± 2.18	4.94 ± 0.27	7.51 ± 0.42	8.46 ± 0.80
1.0	0.71 ± 0.23	$0.93 \pm 0.29^{\#}$	2.11 ± 0.02	$2.88 \pm 0.35^{\#}$	3.98 ± 0.90	5.02 ± 1.06
2.5	0.23 ± 0.08	0.41 ± 0.12	1.32 ± 0.09	$1.41 \pm 0.11^{\#}$	2.08 ± 0.33	2.46 ± 0.30

* : Thresholds of instant redness by observation within 1 min.

** : Thresholds of apparent persistent redness of the skin visible at 48 hours after irrdiation.

$^{\#}$: Estimated without using probit fit.

Microscopic Observations of Skin

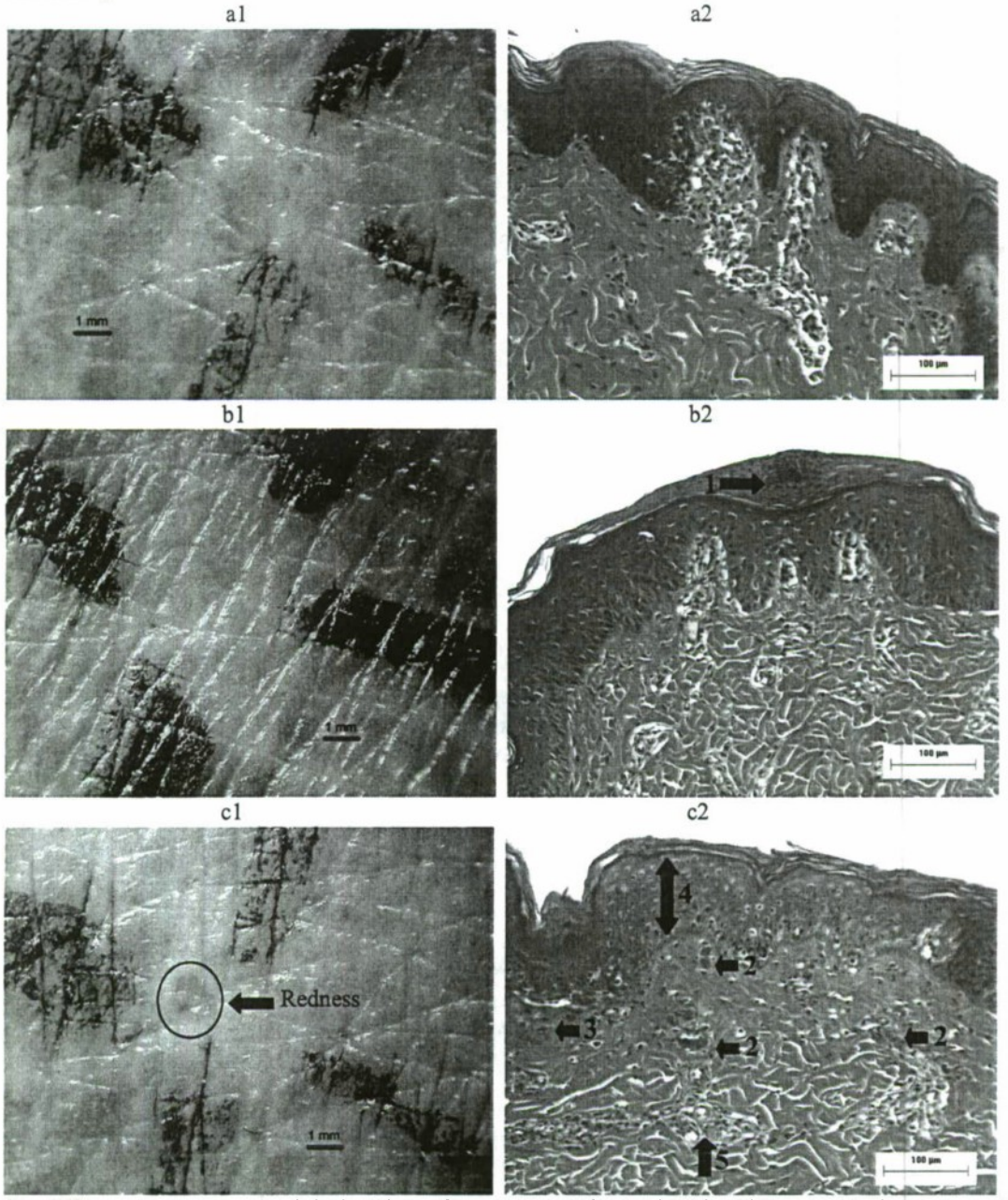

Fig. 5 The gross pictures of mini-pig skin surface 48 hours after various irradiation and their corresponding microscopic biopsies (H&E stain. Mag. 20X). a1,2: no irradiation. b1,2: exposure power around instant redness threshold. c1,2: exposure power at persistent redness threshold. In b2 note: Focal hyperkeratosis (1). In c2 note: Vascular dilation and thrombosis in dermal blood vessels (2), Regenerated epidermis cells (3), transmural necrosis of epidermis (4), and perivascular inflammation (5).

A gross image of persistent redness is showed in Fig.5:c1. Thermal lesion formed flat red papules concomitantly with the shrinking of the epidermis at the center of irradiation sites. The microscopic image of injury is illustrated in Fig.5:c2. There was coagulative necrosis of varying depth at the burn site with loss of epidermis covering some of the more severe burns. The pattern of necrosis was roughly the shape of a flattened cone. Epidermis cells had pyknotic or

shrunken dense nuclei or occasionally fragmented nuclei. Regenerated epidermis cells formed underneath the dead epidermis cells at the lesion boundary. In dermis, some cellular elements were more sensitive to injury than others. They were necrotic at a greater depth than resistant tissues. Thus there was no sharp edge to the burn lesion. The blood vessel endothelium and supporting tissue were more sensitive than other tissues. The vascular dilatation and thrombosis in dermal blood vessels was observed while perivascular inflammation happened in deeper blood vessels.

4 DISCUSSION

The laser powers for ED_{50} thresholds for instant and persistent redness at the sites of irradiation are compared in Table 2. Overall the laser powers for instant redness thresholds were lower than persistent redness thresholds. The gross observation also found that: At some sites irradiated with powers around the instant redness thresholds, redness developed on the skin right after the irradiation but gradually disappeared after several hours.

Histologically, the instant and persistent redness observed on the skin suggests different damage mechanisms. The laser induced temperature rise in the skin results in the dilation of the blood vessel and increasing numbers of open vessels in the dermis. Increased blood perfusion transfers more heat out of the high temperature region to cool the skin to normal temperature.

Instant redness due to hyperhemia was a reversible injury, and the skin with instant redness reverted to its normal state after a few hours without any persistent damage. The H&E stained biopsies of skins where redness appeared right after irradiation with no redness after 48 hours did not present any evidence of persistent injury (Fig.5:b1 and b2). At some higher input power, temperature increased to some critical point where the irreversible redness damage was generated. In other words, persistent redness observed 48 hours after irradiation represented more serious thermal injury to the skin. At persistent redness thresholds, 2000 nm wavelength laser irradiation produced death and necrosis of the epidermis cells and thermal damage to blood vessels leading to a complex series of physiological vascular responses to heating including 1) hemostasis (blood flow stasis), 2) thrombosis and 3) vascular dilatation (Fig.5:c1 and c2). Cells in the upper dermis shrunk and some inflammatory cells were necrotized. The collagen bundles below the epidermis were swollen but there was no change in birefringence image intensity, a sign of heat induced collagen protein denaturation. [21]

It is usually assumed that infrared radiations at wavelengths above 1.4 μm are absorbed in a thin surface layer of the skin, thereby heating the tissue, and inducing an injury as the temperature increases. The conversion of radiant energy to thermal energy can produce damage which can be predicted using the standard rate process model:

$$\Omega = \int_0^{\tau} A e^{-\left[\frac{E}{RT(t)}\right]} dt, \tag{4}$$

where Ω is a dimensionless damage parameter, τ is the exposure time, A is the pre-exponential frequency factor, E is an energy barrier molecules surmount in changing from native state to denatured, R is the gas constant and T is the temperature [15]. The damage parameter Ω indicates the serious level of thermal injury on the skin, and, in this experiment, is set to be 1 for a second degree burn indicated by a persistent red papule at 48 hours.

The ANSI standard of MPE for skin exposure to 2000 nm laser and the experimental results of average energy fluence at ED_{50} damage threshold at various durations and beam sizes are compared in Table 3. Since the MPE level is established for a limiting aperture of 3.5 mm at this wavelength and these exposure durations, the larger spot sizes of our experiment provided additional data for the specification of safety standards for large spots. Table 3 displays the threshold energy divided by the laser spot area. The ED_{50} values for the four exposure times are slightly less than 10 times the corresponding MPEs but not inconsistent considering the inversely proportional size-dependence of ED_{50} values. Based on the experimental data, we can predict that the average energy fluence at ED_{50} damage thresholds for 3.5 mm diameter laser is about ten times larger than MPE standard. Secondly, over the range of exposures, the MPE is larger than one tenth of the damage threshold. It means this MPE standard must be considered carefully and could be decreased as the beam diameter becomes larger than 3.5 mm. In conclusion, this experiment supports the need to reduce the MPE standard for NIR laser beams with 5 mm ~ 15 mm diameter.

TABLE 3. The Average Radiant Exposure [J/cm^2] at ED_{50} Damage Thresholds

Diameter (mm) / Duration(s)	4.83	9.65	14.65	3.5 (MPE from ANSI)
0.25	3.57 ± 0.38 J/cm^2	2.89 ± 0.36 J/cm^2	2.39 ± 0.06 J/cm^2	0.396 J/cm^2
0.5	4.07 ± 1.31 J/cm^2	3.38 ± 0.18 J/cm^2	2.51 ± 0.24 J/cm^2	0.471 J/cm^2
1.0	5.08 ± 1.58 J/cm^2	3.94 ± 0.48 J/cm^2	2.98 ± 0.63 J/cm^2	0.560 J/cm^2
2.5	5.59 ± 1.64 J/cm^2	4.82 ± 0.38 J/cm^2	3.65 ± 0.44 J/cm^2	0.704 J/cm^2

One thing to be noted is that the laser beam diameter for non uniform beam profile are typically quoted at 1/e rather than 1/e^2 to give more conservative radiant exposures to compare to published MPE values in the laser safety classification. The radiant exposure based on 1/e diameter is just twice as large as the 1/e^2 diameter radiant exposure, and indicates the peak radiant exposure for Gaussian shape laser beam. Although 1/e diameter is a conservative estimation of the laser hazard classification, 1/e^2 diameter must be used to truly evaluate laser damage thresholds which require average irradiance.

The average irradiance and exposure duration at ED_{50} damage threshold was investigated based on the power law relation postulated by Stoll and Greene in 1959 [22]. They investigated the relationship between pain and tissue damage due to white light irradiation using three human subjects. Based on the data they acquired a simple irradiance-time power law:

$$E = A\, t^{-B}, \tag{5}$$

was found, where A and B are positive constants, E is the irradiance at the threshold and t is the exposure duration. Figure 6 clearly shows that the irradiance-time power law can precisely describe our experimental results of irradiance at ED_{50} damage thresholds. Although coefficient A varies with respect to beam size, the power coefficient B is constant around 0.8, which is close to the Stoll's finding-----B=0.74 for thresholds of pain with burning. For a spot diameter around 15 mm, which is used in Stoll's experiment as well, the power law for laser induced lesion is given by $E = (3.07\ \mathrm{W/cm^2})t^{-0.81}$. This is close to Stoll's finding when the skin tissue was irradiated by a white light projection lamp yielding an irradiance-time power law of $E = (2.82\ \mathrm{W/cm^2})\, t^{-0.74}$. Power law coefficient A for various spot diameters are examined in Figure 7. A least square linear fit indicates there is a simple relationship between coefficient A and spot diameter d(cm) ------ A =5.669 -1.81d (Fig. 7). In conclusion, the irradiation at the ED_{50} damage threshold could be predicted by this empirical equation $E = (5.669 - 1.81d)t^{-0.794}$ (W/cm^2). Recalling the MPE standard and that the standard is a factor of ten lower than threshold, the MPE radiant exposure is $H = 0.56t^{0.25}$ (J/cm^2). For spot diameter equals 0.35 cm, the empirical power law gives a close estimation $H = 0.50t^{0.206}$ (J/cm^2) (define the MPE radiant exposure as one tenth of the radiant exposure at the ED_{50} damage threshold.). For d=1.465 cm, the MPE radiant exposure from our estimation should be $0.302t^{0.206}$ (J/cm^2). Although the empirical equation $E = (5.669 - 1.81d)t^{-0.794}$ (W/cm^2) fits our threshold results quite well, it is obviously not suitable for much smaller or larger spot sizes. For spot diameters much larger than 15 mm, the irradiance at threshold should be independent of the spot size. On the other hand, for smaller spot diameters much less than 5 mm, the threshold irradiance will increase faster than this linear prediction [23,24]. For instance, McCally *et al.* [13] measured the cornea epithelial damage thresholds for 0.235 s exposure and 1.33 mm 1/e^2 spot diameter at wavelength 2.02 μm. The measured threshold radiant exposure was 8.46 J/cm^2 which is higher than the predicted value 4.03 J/cm^2 from

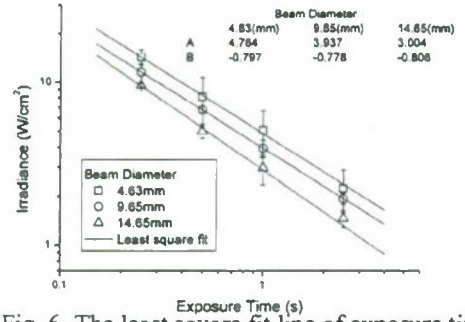

Fig. 6. The least square fit line of exposure time and irradiance, E_T=A t^B

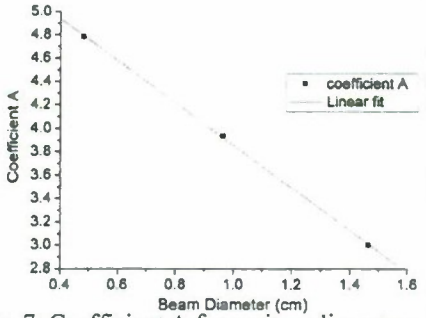

Fig. 7. Coefficient A for various diameters (d(cm)). Linear fit shows A = 5.669 – 1.81d

our linear empirical equation.

5 CONCLUSION

We have measured the minimum visible lesion thresholds in Yucatan mini-pig skin for three different laser spot sizes at four various pulse durations. For a CW 2000 nm wavelength laser, the irradiance exposure-time power-law has been evaluated based on the experimental results of the average irradiance values at the thresholds. It shows that the average irradiance at the ED_{50} damage threshold has a simple power law relation to exposure time $E = (5.669 - 1.81d)t^{-0.794}$ (W/cm^2). This simple empirical equation reveals the duration and size dependences of the ED_{50} damage thresholds. For Gaussian shape laser irradiation, which is common in many laser medical applications, lower energy is needed to generate a lesion on skin for smaller spot sizes and shorter exposure durations. On the other hand, the average radiant exposure at threshold is inversely proportional to spot size. These effects occur due to the Gaussian shape of the laser beam and the heat transfer during irradiation.

We calculate the MPE from ANSI standards for 2000 nm wavelength at the exposure duration used in the experiments and conclude that the MPE standard is reasonable for the original 3.5mm spot diameter, but larger than necessary for 4.83 mm, 9.65 mm and 14.65 mm spot sizes and exposure durations of 0.25 second and longer. For our criterion of damage, the MPEs are bigger than one tenth of ED_{50} damage thresholds, therefore the MPE standard should be considered carefully and could be decreased as the laser beam diameter becomes larger than 3.5 mm.

ACKNOWLEDGMENTS

Opinions, interpretations, conclusions, and recommendations are those of the authors and are not necessarily endorsed by the University of Texas, the United States Air Force or the Department of Defense.

The authors wish to thank Dr. Darrell Tata, Dr. Robert J. Thomas, Dr. Sergey Telenkov, Victor Villavicencio, Dan Polhamus and Jennifer Cassaday for their kind help.

Contract grant sponsor: Northrop Grumman Information Technology; Contract grant sponsor: The Albert and Clemmie Caster Foundation.

REFERENCES

1. Trauner K, Nishioka N, Patel D. Pulsed holmium:yttrium-aluminum-garnet (Ho:YAG) laser ablation of ®brocartilage and articular cartilage. Am J Sports Med 1990; 18(3):316-320.
2. Trauner KB, Nishioka NS, Flotte T, Patel D. Acute and chronic response of articular cartilage to holmium:YAG laser irradiation. Clin Orthop 1995; 310:52-57.
3. Gerber BE, Asshauer T, Delacretaz G, Jansen T, Oberthur T. Biophysical bases of the effects of holmium laser on articular cartilage and their impact on clinical application technics. Orthopade 1996; 25(1):21-29.
4. Yiu MK, Liu PL, Yiu TF, Chan AYT. Clinical experience with holmium:YAG laser lithotripsy of ureteral calculi. Lasers Surg Med 1996; 19:103–106.
5. Razvi HA, Denstedt JD, Chun SS, Sales JL. Intracorporeal lithotripsy with the holmium:YAG laser. J Urology 1996; 156:9-12.
6. Das A, Erhard MJ, Bagley DH. Intrarenal use of the holmium laser. Lasers Surg Med 1996; 19:103–106.
7. Oswal VH, Bingham BJG. A pilot study of the Holmium YAG laser in nasal turbinate and tonsil surgery. J Clin Laser Med Surg 1992; 10:211-216.
8. Shapshay SM, Rebeiz EE, Pankratov MM. Holmium: Yttrium Aluminium Garnet laser-assisted endoscopic sinus surgery: clinical experience. Laryngoscope 1992; 102:1177-1180.
9. Shapshay SM, Rebeiz EE, Bohigian RK. Holmium: Yttrium Aluminium Garnet laser-assisted endoscopic sinus surgery: laboratory experience. Laryngoscope 1991; 101:142-149.
10. Min K, Leu H, Zweifel K. Quantitative determination of ablation in weight of lumbar intervertebral discs with Holmium:YAG laser. Lasers Surg Med 1996; 18:187–190
11. American National Standards Institute, ANSI Z136.1-2000, American National Standard for Safe Use of Lasers. Laser Institute of America, Orlando, FL, 2000
12. Lund DJ, Beatrice ES, Stuck BE, Biological Research in Support of Project MILES, Letterman Army Institute of Research Report- Institute Report No. 96, 1981
13. McCally RL, Farrell RA, Bargeron CB, Cornea epithelial damage thresholds in rabbits exposed to Tm:YAG laser radiation at 2.02 microns, Lasers Surg Med 1992; 12:598-603
14. Sliney D, Wolbarsht M. Safety with Lasers and Other Optical Sources. New York; Plenum Press. 1980

15. Henriques FF. Studies of thermal injury V. Archives of Pathology. 1947; 43:489-502
16. Takata A.N. Laser-induced thermal damage of skin. USAF School of Aerospace Medicine, Brooks Air Force Base, TX. 1977
17. Eggleston TA, Roach WP, Mitchell MA, Smith K, Oler D, Johnson TE. Comparison of two porcine (Sus scrofa domestica) skin models for in vivo near-infrared laser exposure. Comp Med. 2000; 50(4):391-397.
18. Siegman AE, Sasnett MW, Johnston JTF. Choice of clip levels for beam width measurements using knife-edge techniques. IEEE J. Quantum Electron. 1991; 27:1098-1104
19. Finney DJ,. Probit Analysis. 3rd ed., New York; Cambridge University Press. 1971
20. Cain CP, Noojin GD., A Comparison of Various Probit Methods for Analyzing Yes/No Data on a Log Scale. Brooks AFB, TX: USAF Armstrong Laboratory; AL/OE-TR-1996-0102; 1996
21. Thomsen SL. Qualitative and quantitative pathology of clinically relevant thermal lesions: In Matching the Energy Source to the Clinical Need. pp. 425–459. SPIE Publishers, Bellingham, WA, 1999.
22. Stoll AM, Greene LC. Relationship between pain and tissue damage due to thermal irradiation. J App. Physiology. 1959; 14(3):372-382
23. Tan OT, Motemedi M, Welch AJ, Kurban AK. Spotsize effects on guinea pig skin following pulsed irradiation. J Invest. Dermatol. 1988; 90(6): 877-881
24. Keijzer M, Pickering JW, van Gemert MJC. Laser beam diameter for port wine stain treatment. Lasers Surg Med 1991; 11:601-605